Functional Imaging of Photosensitizers using Multiphoton Microscopy

Eric Wachter*, Craig Dees, Jay Harkins, Walt Fisher and Tim Scott
Photogen, Inc., Knoxville, TN 37931 USA

ABSTRACT

Multiphoton imaging of the sub-cellular distribution of photosensitizers can provide important clues to their mechanism of action in tumors. We have used this tool to study distribution and pharmacology of photosensitizers in murine hepatoma tumor cells dosed with various photosensitizers. Upon photoactivation, Rose Bengal yields nearly immediate photolytic release of lysosomal enzymes, resulting in catastrophic cell destruction within 5-30 minutes. Such marked response is quite different than that observed with other photosensitizer agents, and is consistent with *in vivo* studies illustrating that Rose Bengal is capable of causing extremely rapid destruction of treated tumors.

Keywords: photosensitizer, microscopy, imaging, multiphoton, MPE, ultrafast, femtosecond

1. INTRODUCTION

The number of reported applications for multiphoton excitation (MPE) in microscopic imaging of biological systems is rapidly expanding for several very good reasons: MPE causes minimal photo-bleaching and photo-damage of the sample; it affords greatly reduced interference from scatter in optically dense media; and it offers exceptional spatial resolution, particularly along the optical axis.[1-3] An area of particular interest to us is imaging of the sub-cellular pharmacology of photosensitizers in tumor cells. The ability to readily resolve sub-cellular membranes and organelles, coupled with the low photo-damage potential of MPE, facilitates prolonged study of the pharmacokinetics and pharmacology of photosensitizers in living cells, tissue cultures, and tissue specimens.

Our model compound for these studies is Rose Bengal (4,5,6,7-tetrachloro-2',4',5',7'-tetraiodofluorescein disodium, or "RB"), a potent anionic, amphipathic photosensitizer capable of photocatalytic conversion of triplet oxygen ($^3O_2$) to singlet oxygen ($^1O_2$*).[4-10] RB has an extremely large cross-section (E_M = 99,800 $\underline{M}^{-1}$ cm^{-1} at 549 nm in water) and its photochemical properties exhibit minimal sensitivity to the local environment (*i.e.*, # 10 nm spectral shift between hydrophilic and hydrophobic media).[6,8] A combination of high intersystem crossing quantum yield and singlet oxygen yield leads to highly efficient $^1O_2$* production upon irradiation with green light. Moreover, RB readily photobleaches to an inactive state,[11] suggesting that its photodynamic effects may be self-limiting. While the large singlet oxygen quantum yield suggests that RB is a poor candidate for use as a fluorescent dye, it nonetheless exhibits sufficient luminescence to enable direct visualization under single-photon excitation or MPE.

Thus, we report here recent work with the photosensitizer Rose Bengal, imaged in tissue cell culture. Using photoactivation with green light, we are able to assess the sub-cellular basis for the unique photosensitizing properties of the agent. These properties are compared with other photosensitizers, such as Rhodamine 6G and 123, and placed into context relative to *in vivo* outcome.

*Correspondence: wachter@photogen.com; phone 1 865-769-4011; fax 1 865-769-4013; http://www.photogen.com

2. METHODOLOGY

2.1 MPE Microscopy

A titanium sapphire (Ti:S) laser (Coherent, Model 900F) mode-locked at ca. 80 MHz, with a pulse width of ca. 100 femto-seconds, was used to excite samples at 800 nm using an average power of ca. 5-20 mW. Light from this ultrafast laser was directed to samples using a non-descanned inverted microscope (similar to that described by Piston et al.[12]) constructed around a high-NA objective (Olympus UPlanFL, 100X / 1.3 N.A.) and dual-axis galvanometer system (Model 6210, Cambridge Technology Incorporated). In addition, a cw laser (Coherent Verdi-V5-OEM, 532 nm) was used for photosensitizer activation; light from this second laser was delivered to the sample using a GRIN microlens fiberoptic diffuser (Pioneer Optics). Data acquisition and sample photoactivation were automated using proprietary system control software.

2.2 Sample Preparation

Tissue cultures (murine hepatoma cells, Hepa 1-6, ATCC CRL-1830) were prepared on Nunc coverslip slides, and were treated with aqueous photosensitizer (RB; Rhodamine 6G, i.e., "R6G"; or Rhodamine 123, i.e., "R123", at concentrations ranging from 0.001% to 0.1%) for ca. 30 min immediately prior to use. Treated cells were then washed with fresh growth media. Reference stains (i.e., LysoSensor Green, Ethidium Homodymer-1, Hoechst 33342) were added in various combinations to enable observation of changes in sub-cellular structure via MPE microscopy.

3. DATA AND DISCUSSION

The cationic Rhodamines and anionic RB exhibited interesting sub-cellular localization, however the target structures appear to be quite different, as illustrated in Figures 1-3. This compartmentalization is further demonstrated in Figures 4-6, which illustrate RB localization within the cytoplasmic volume and complete exclusion from the nucleus.

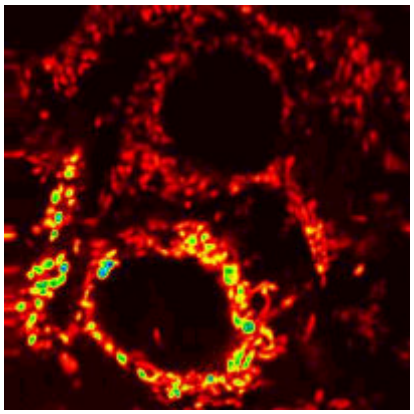

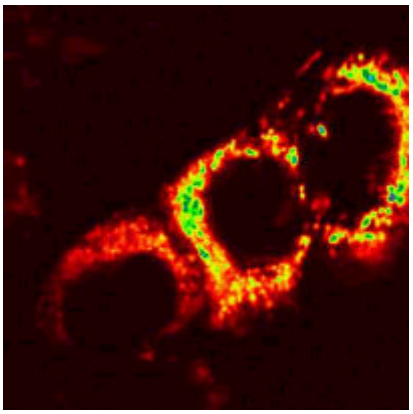

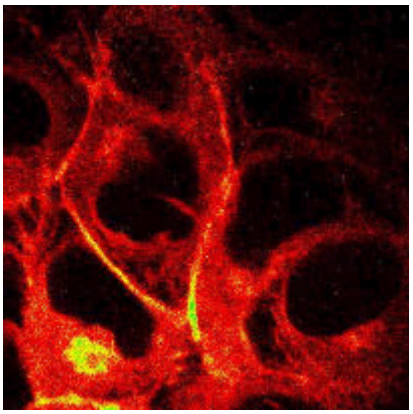

Figure 1 (left). MPE image of hepatoma cells (grown in cell culture) following treatment with 2.5 µg/mL aqueous R6G. Internalization of the cationic agent in mitochondria and exclusion from the nucleus is evident. Note also absence of staining of cellular membranes.

Figure 2 (center). MPE image of hepatoma cells following treatment with 10 µg/mL aqueous R123. As in the case of R6G, internalization of the agent in mitochondria and exclusion from the nucleus is evident.

Figure 3 (right). MPE image of hepatoma cells following treatment with 10 µg/mL aqueous RB. In contrast to the Rhodamines, RB appears to be internalized in the cell membrane and other internal membranes; exclusion from the nucleus is also evident.

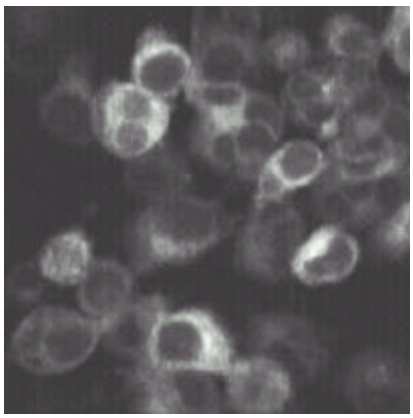

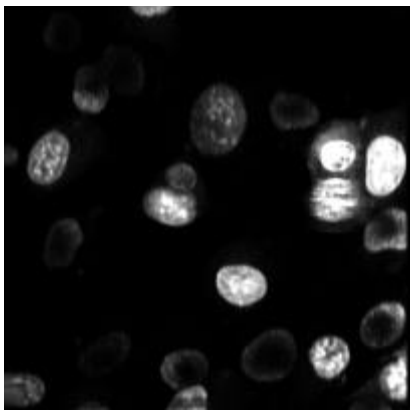

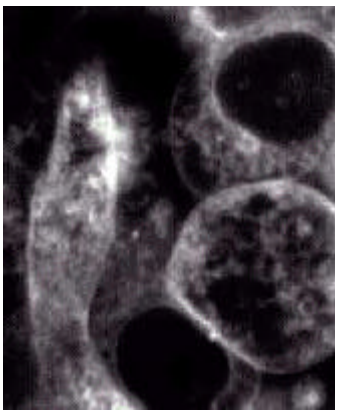

Figure 4 (left). MPE image of hepatoma cells (grown in cell culture) following treatment with aqueous aqueous RB. RB internalization in all cells is evident with confinement to the cell membrane and other internal structures.

Figure 5 (center). MPE image of hepatoma cells following staining with Hoechst 33342 nuclear stain. Clear demarcation of the nucleus is evident upon comparison with the RB-stained image (Figure 4).

Figure 6 (right). Close-up image of hepatoma cells following treatment with aqueous RB. Marked concentration and organization of RB within the cytoplasmic volume is evident.

Mitochondrial staining, such as that observed for the Rhodamines, is known to precipitate an apoptotic response upon photoactivation. Illumination of cell cultures treated with R6G or R123 yielded minimal immediate effect, consistent with such a mechanism.

In contrast, staining with anionic RB yielded immediate, marked effects, as illustrated in Figure 7. In this series of images, hepatoma cells were pre-treated with RB, then briefly illuminated with light at 532 nm to photoactivate the RB; the resultant effects are seen upon comparison of the pre- and post-illumination images. The cells were counter-stained prior to imaging using LysoSensor Green (LSG, which stains intact lysosomes and is visible in the blue detector channel) and Ethidium Homodymer-1 (ED-1, which is excluded from intact nuclei, but becomes visible in the red detector channel if nuclear integrity is lost); both vital stains were present throughout the duration of the experiment, and do not appear to cause photosensitization. The sequence is organized in two sets of columns, illustrating simultaneously acquired images from the red detector channel on the left and the blue detector channel on the right of each column; elapsed time increases down each column starting at the upper left corner of the figure.

In the initial pair of images (Figure 7, upper left, obtained immediately prior to illumination with green light), the cells exhibit intra-cellular staining with RB but no nuclear staining by either RB or ED-1 (red channel); the blue channel exhibits a distinctive pattern of lysosomal staining with LSG. The second pair of images represent the cells immediately post-illumination (i.e., after 30 s illumination with 532 nm light, ca. 250 mW/cm^2), and show little effect. However, by the third time point (1.5 min post-illumination), significant loss of lysosomal integrity is evident in the blue channel. At 10 min, further loss of lysosomal integrity is noted, coupled with greatly diminished cytoplasmic signal in the red channel; morphologic changes also begin to appear, along with evidence of ED-1 leakage into the nuclei. By 15 min, large intra-cellular voids begin to appear, which grow progressively more pronounced at 20 and 25 min; increased nuclear staining is also noted over this period. At 30 min post-illumination, catastrophic loss of integrity is noted in one of the imaged cells, characterized by marked nuclear staining and dramatic change of cell morphology. Between 35 and 40 min post-illumination, the other imaged cell exhibits similar catastrophic changes.

The dramatic changes noted in Figure 7 appear to be the consequence of massive photolytic release of lysosomal contents upon photoactivation of RB, which has a proclivity for concentration in lysosomes due to its anionic nature. Such photolytic release leads to rapid autolysis of the hepatoma cells.

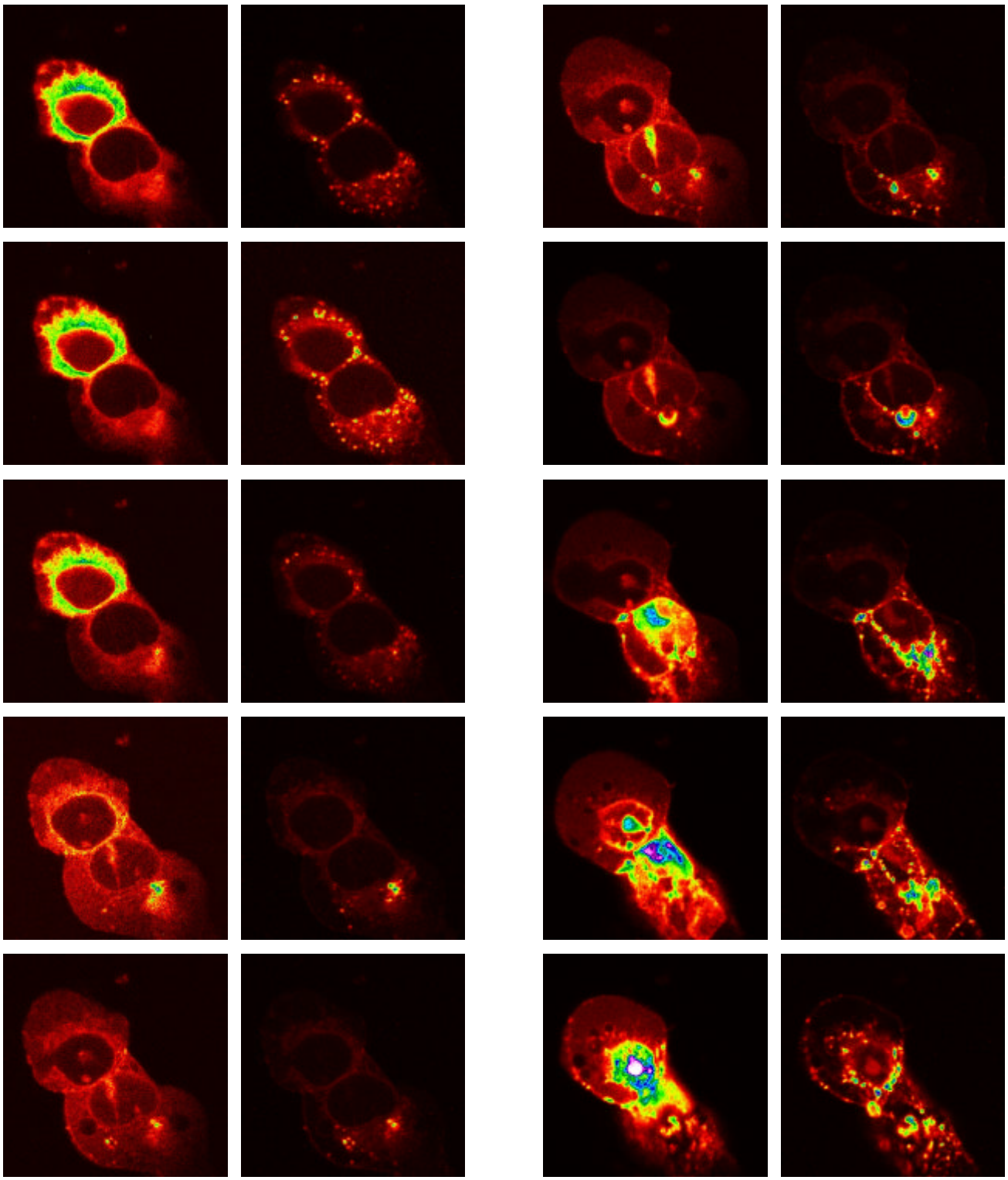

Figure 7. Hepatoma cells pre-treated with RB, then briefly illuminated at 532 nm; cells were counter-stained prior to imaging using LSG and ED-1. The sequence, starting at upper left, is organized sequentially in two sets of columns, illustrating paired red (left) and blue (right) detector channels in each column. Elapsed time: pre-illumination, 0.5, 1.5, 10, 15, 20, 25, 30, 35, and 40 min post-illumination.

The severity of this "photolysis" effect, at the cellular level, appears to be much greater, with a far more rapid onset, than is seen with other photosensitizers (such as the Rhodamines). For example, implanted murine tumors treated with RB typically exhibit signs of localized liquification within several hours of illumination, forming flat, dry eschars within at 24-h post-treatment (Figure 8).

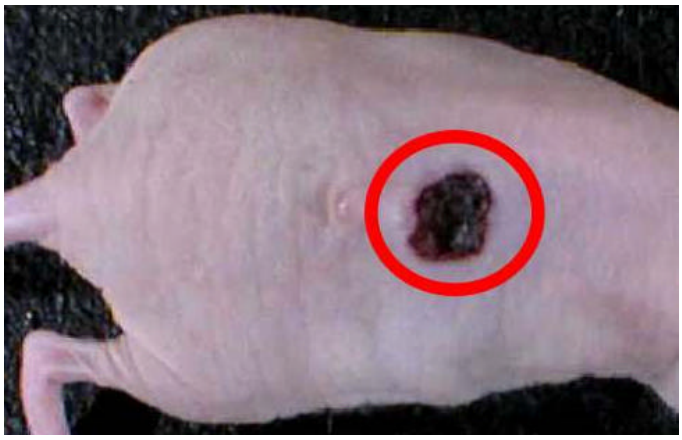

Figure 8. An implanted renal adenocarinoma tumor in an athymic nude mouse, 24-h post photodynamic treatment using oral RB. Tumor treated with 100 J/cm^2 light at 532 nm following administration of RB. Circle shows illuminated area. The flat, dry eschar encompasses the entire tumor. We have found such response to be typical when using RB.

5. CONCLUSIONS

Multiphoton microscopy enables prolonged, quasi-continuous imaging of the sub-cellular distribution of photosensitizers within in living cells. The method has allowed us to observe that, upon photoactivation, Rose Bengal yields nearly immediate photolytic release of lysosomal enzymes, resulting in catastrophic cell destruction within 5-30 minutes; similar *in vivo* effects are seen in implanted murine tumors.

REFERENCES

1. M.J. Wirth and F.E. Lytle, "Two-photon excited molecular fluorescence in optically dense media," *Anal. Chem.*, **49**, pp. 2054-2057, 1977.
2. W. Denk, J.H. Strickler and W.W. Webb, "Two-photon laser scanning microscopy," *Science*, **248**, pp. 73-76, 1990.
3. D.W. Piston, M.S. Kirby, H. Cheng, W.J. Lederer, and W.W. Webb, "Two-photon excitation fluorescence imaging of three-dimensional calcium ion activity," *App. Opt.*, **33**, pp. 662-669, 1994.
4. T. Ito and K. Kobayashi, "A survey of in vivo photodynamic activity of xanthenes, thiazines, and acridines in yeast cells," *Photochem. Photobiol.*, **26**, pp. 581-587, 1977.
5. S.A. Bezman, P.A. Burtis, T.P.J. Izod and M.A. Thayer, "Photodynamic inactivation of E. coli by rose bengal immobilized on polystyrene beads," *Photochem. Photobiol.*, **28**, pp. 325-329, 1978.
6. N. Houba-Herin, C.M. Calberg-Bacq, J. Piette and A. Van de Vorst, "Mechanisms for dye-mediated photodynamic action: singlet oxygen production, deoxyguanosine oxidation and phage inactivating efficiencies," *Photochem. Photobiol.*, **36**, pp. 297-306, 1982.
7. J. Paczkowski, J.J.M. Lamberts, B. Paczkowska and D.C. Neckers, "Photophysical properties of rose bengal and its derivatives," *J. Free Rad. Biol. Med.*, **1**, pp. 341-351, 1985.
8. D.C. Neckers, "Rose bengal," *J. Photochem. Photobiol.*, **47**, pp. 1-29, 1989.
9. I.E. Kochevar, C.R. Lambert, M.C. Lynch and A.C. Tedesco, "Comparison of photosensitized plasma membrane damage caused by singlet oxygen and free radicals," *Biochim. Biophys. Acta*, **1280**, pp. 223-230, 1996.
10. P.C. Lee and M.A.J. Rodgers, "Laser flash photokinetic studies of rose bengal sensitized photodynamic interactions of nucleotides and DNA," *Photochem. Photobiol.*, **45**, pp. 79-86, 1987.
11. Y. Tonogai, Y. Ito, M. Iwaida, M. Tati, Y. Ose and T. Sato, "Studies of the toxicity of coal-tar dyes. I. Photodecomposed products of four xanthene dyes and their acute toxicity to fish," *J. Toxicol. Sci.*, **4**, pp. 115-125, 1979.
12. D.W. Piston and S.M. Knobel, "Quantitative imaging of metabolism by two-photon excitation microscopy," in: *Methods in Enzymology, Confocal Microscopy, Chapter 21, Vol. 307*, P.M. Conn (ed). Academic Press, New York, pp. 351-368, 1999.

Functional Imaging of Photosensitizers using Multiphoton Microscopy

Eric Wachter, Craig Dees, Jay Harkins, Walt Fisher and Tim Scott
Photogen, Inc., Knoxville, TN 37931 USA

ABSTRACT

Multiphoton imaging of the sub-cellular distribution of photosensitizers can provide important clues to their mechanism of action in tumors. We have used this tool to study distribution and pharmacology of photosensitizers in murine hepatoma tumor cells dosed with various photosensitizers. Upon photoactivation, Rose Bengal yields nearly immediate photolytic release of lysosomal enzymes, resulting in catastrophic cell destruction within 5-30 minutes. Such marked response is quite different than that observed with other photosensitizer agents, and is consistent with *in vivo* studies illustrating that Rose Bengal is capable of causing extremely rapid destruction of treated tumors.

Keywords: photosensitizer, microscopy, imaging, multiphoton, MPE, ultrafast, femtosecond

In:
Multiphoton Microscopy in the Biomedical Sciences II
SPIE Paper **4620-29**
BiOS 2002 (Biomedical Optics), San Jose, CA
21 January 2002